Evolution of the cathode spot distribution in an axial magnetic field controlled vacuum arc at long contact gap

B. Tezenas Du Montcel, P Chapelle, A. Jardy, C. Creusot

EVOLUTION OF THE CATHODE SPOT DISTRIBUTION IN AN AXIAL MAGNETIC FIELD CONTROLLED VACUUM ARC AT LONG CONTACT GAP

B. Tezenas du Montcel[a,b], P. Chapelle[a,*], A. Jardy[a], C. Creusot[b]

[a] *Institut Jean Lamour - UMR 7198 CNRS/Université de Lorraine, Laboratoire d'Excellence DAMAS, CS 50840, 54011 Nancy Cedex, FRANCE*

[b] *SuperGrid Institute SAS, 130 rue Léon Blum, BP1321, 69611 Villeurbanne, FRANCE*

[*] pierre.chapelle@univ-lorraine.fr

Abstract. The distribution of cathode spots in a CuCr25 vacuum arc controlled by an axial magnetic field and ignited on the lateral surface of the cathode is investigated for long gap distances, from the processing of high-speed video images. The processing method includes also estimating the current carried by a single spot and reconstructing the distribution of the current density at the cathode. Various distributions depending partly on the arc current are described.

Keywords: Vacuum arc, Axial magnetic field, Long gap, Cathode spot distribution, Experimental study.

1. Introduction

Vacuum is one of the most frequently extinguishing medium for medium voltage circuit breakers. At relatively low current or under an axial magnetic field (AMF), a vacuum arc (VA) appears diffuse. The plasma is provided at the cathode by tiny, mobile cathode spots (CS) [1]. CS motion is influenced by various factors, such as surface state, magnetic field and the plasma density near the cathode [2]. The distribution of CSs over the cathode surface has obviously a strong impact on the plasma parameters [3].

Using a numerical processing method of cathode spot images [4], two groups of authors succeeded reconstructing the position of CSs over the cathode surface, from which they have studied the distribution of current density at the cathode [5, 6] and the extension of the area occupied by CSs [2, 7]. These experiments were conducted between static contacts. The arc was triggered thank to an auxiliary electrode inserted at the center of the cathode. Only short contact gaps ranging from 4 to 6 mm in [2, 5, 7] or equal to 11 mm in [6] were considered, with maximal current in 7–25 kA range.

Current efforts to enhance the vacuum circuit breaker voltage range capability impose to employ higher contact gaps (more than 10 mm). However, VA behavior under such conditions is still not fully understood. In this paper, based on a similar method to [4], we investigate the distributions of cathode spots and current density at the cathode in AMF controlled VAs generated between static contacts spaced 20 mm or 30 mm apart, and triggered with an auxiliary electrode situated near the cathode lateral surface. Different evolutions of the CS distribution, mainly depending on the VA current, are described and analyzed.

2. Experimental

2.1. Experimental setup

The experimental setup, illustrated in Figure 1, is composed of a vacuum chamber (10^{-5}–10^{-7} Pa) inside which two fixed 70 mm diameter copper cylindrical contacts surmounted by CuCr25 wafers are mounted. Sixteen turn Helmholtz coils (HC) disposed outside the chamber are used to generate an AMF. As it can be seen in Figure 2, the radial profile of the AMF has a saddle shape with values of 9.6–17.1 mT/kA inside the contact gap region. On the contrary, the time delay between the AMF intensity and the coil current has a bell-shaped radial profile, with values ranging between 3.4 ms and 5.4 ms inside the contact gap region. VA is triggered with the help of an auxiliary electrode situated close to the lateral surface of the cathode and connected to a microsecond High-Voltage (HV) power supply. VA and HC are powered from two independent 50 Hz alternators. A phase shift of 3.4 ms is imposed between the coil current and the arc current to synchronize the AMF and arc current peaks at the edge of the contacts. VAs are filmed with a high-speed camera Photron SA5 with an exposure time of 369 ns and a frame rate in 15000–20000 fps.

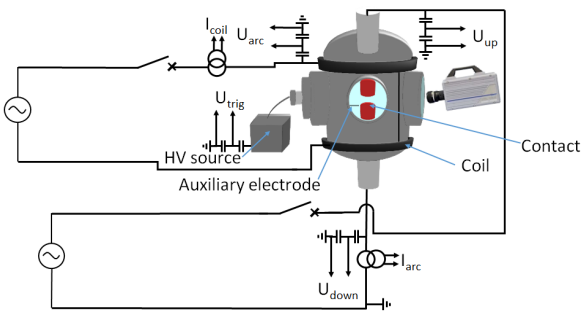

Figure 1. Experimental setup.

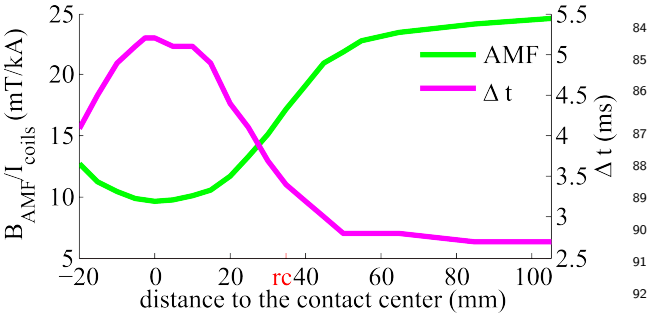

Figure 2. Radial profiles of the axial magnetic field intensity and the time delay (Δt) between B_{AMF} and I_{coil} measured at mid distance between the two contacts.

2.2. Operating parameters

Table 1 shows the operating parameters used during the eleven experiments that are reported in the present paper. Arc current is in 4.9–43.3 kA. All experiments were realized with the AMF oriented towards the cathode, except experiment 7, during which the AMF was oriented towards the anode. The contact gap was either 20 mm or 30 mm.

Experiment	L_{arc} mm	I_{arc} kA	T ms	B_{AMF} mT
1	20	4.9	6.2	-143
2	20	17.2	13.7	-143
3	20	25.7	11.8	-143
4	20	26.7	9.9	-143
5	20	31.1	10.8	-143
6	20	36.3	11.7	-143
7	20	43.3	10.9	269
8	30	8.9	10.9	-145
9	30	11.7	10.9	-144
10	30	18.0	10.9	-143
11	30	24.9	10.9	-141

Table 1. Gap distance, arc current, arc duration and AMF magnitude during each experiment.

2.3. Numerical treatment of cathode spot images

CS distribution was studied with the help of a numerical treatment of cathode spot images developed within the Octave software and inspired by the method proposed by Afanas'ev *et al.* [4]:

1. To detect the CSs, the iso-contours of light intensity on the cathode spot image were calculated with a native function of Octave. Next, these contours were selected according to their intensity, in order to eliminate the darkest contours, as well as according to their size, in order to reject too long and too small contours which cannot surround a single spot. Then, the iso-contour density was estimated by calculating first the centroid position of each contour. When the number of centroids on a pixel reaches a threshold value, this pixel was marked. Finally, spot position was taken as the centroid of connexe area of marked pixels.

2. The image deformation induced by the inclination of the camera was corrected using an OCTAVE native projective transformation function. This function must be supplied with the initial and final positions of four points. For this purpose, we have used the picture of a grid pattern disposed on the cathode surface, which was taken with the same inclination as that during the experiment.

3. From the CS map, the distribution of the current density at the cathode was reconstructed by partitionning the cathode surface into Voronoi cells, each cell enclosing a single spot. The current density in each cell was considered to be inversely proportional to the cell area.

3. Results

3.1. Cathode spots distribution

Because of the lateral trigger system, CSs just after the VA ignition are located on the lateral surface of the cathode. The action of the AMF results then in a very fast retrograde motion of rotation of those spots around the cathode [8]. Eventually, the CSs reach the front surface and spread over it. The temporal evolution of the CS distribution on the cathode surface was investigated using the image processing method described in section 2.3. As shown in Figure 3, various types of evolution of the CS distribution were observed depending partly on the arc current.

1. At low current (up to 11.7 kA for the present conditions, i.e. in Experiments 1, 8 and 9), only a small part of the circumferential edge of the cathode is initially occupied by the cathode spots (Figure 3.a). Subsequently, the occupied area grows in size until the current peak (at around 6 ms). The growth seems to be roughly isotropic as in [2]. The spots form a compact group, and they never manage to fill the whole front surface of the cathode.

2. At moderate current (between 17.2 kA and 31.1 kA for the present conditions, i.e. in Experiments 2 to 5, 10 and 11), the first CSs appearing on the front surface form thin separate strips covering large sections of the cathode circumferential edge (Figures 3.b-c). Next, with the increase of the arc current, the regions occupied by CSs grow along the edge of the cathode, as well as toward the center of the cathode. Eventually, at $t = 4$ ms, the circumference of the cathode is totally covered by the spots, but an empty region is still enclosed within the CS distribution. Then, two types of evolution may be distinguished according to the centering of the empty region with respect to the axis of symmetry of the cathode at $t = 4$ ms:

   a. In Experiments 3 and 4, as illustrated in Figure 3.b, the empty region initially relatively de-

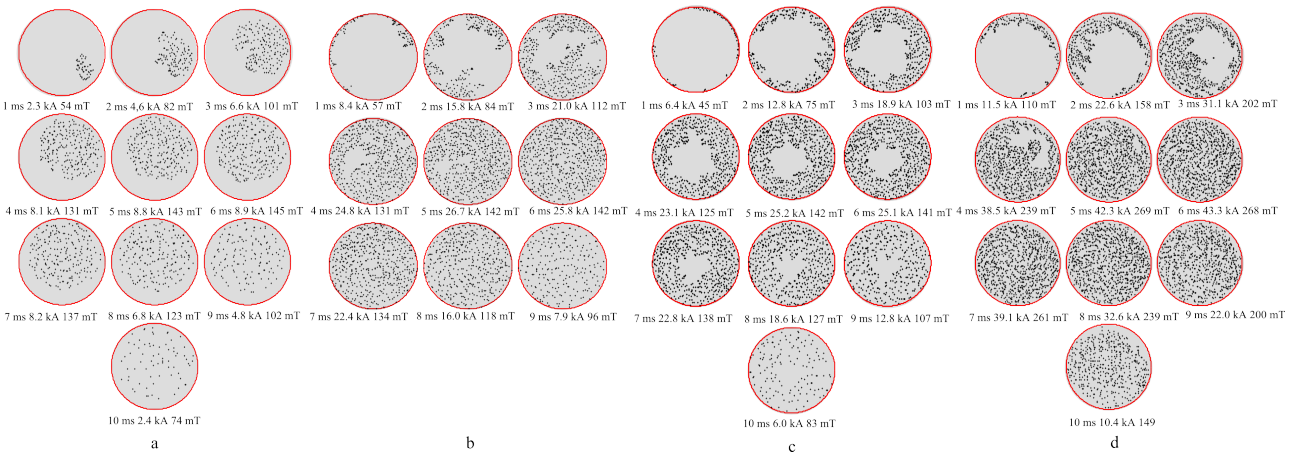

Figure 3. Temporal evolution of the distribution of cathode spots during Experiments (a) 8, (b) 4, (c) 11 and (d) 7.

centered and is eventually totally filled by the spots a delay after the current peak.

b. In Experiments 2, 5 10 and 11, as illustrated in Figure 3.c, the empty region is initially relatively centered, and although its size decreases until the current peak; it remains present until the arc extinction.

3. At high current (above 36.3 kA for the present conditions, i.e. in Experiments 6 and 7), the CS distribution evolves similarly to that at moderate current (Figure 3.d). Yet, at the current peak, the top surface of the cathode is always entirely covered by spots. Moreover, the CS distribution seems to reveal an alignment of the cathode spots along spiral arms originating from the center of the cathode.

Note that in all cases, during the decrease of the arc current, the disappearance of CSs seems to happen uniformly over the cathode surface.

3.2. Cathode spot average current

From the data provided by the spot detection procedure, it is possible to determine the average spot current by calculating the ratio of the total arc current to the number of detected spots. We have excluded from our analysis images where a significant proportion of spots could not be detected by our algorithm, because they were located on the lateral surface of the cathode, as a result of either the arc ignition or the ejection of spots from the front surface. Based on arc images taken 1 ms before the arc extinction, an average spot current value of 36.5 ± 2.5 A was obtained for all experiments. This value is similar to the spot current measured by Yu *et al.* [9] for nanocrystaline CuCr25 contact material.

3.3. Radial profile of the cathode current density

The measured spatial distributions of the cathode spots have been used to reconstruct the distributions of the current density at the cathode surface, following the method described in Section 2.3. Azimuthally averaged radial profiles of the cathode current density corresponding to the spatial distributions of spots presented in Figure 3 are shown in Figure 4.

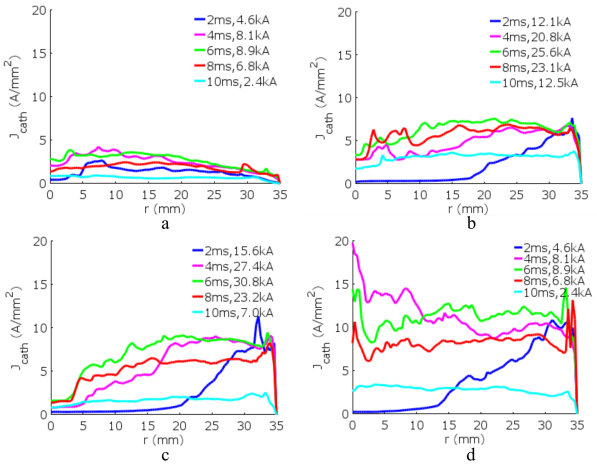

Figure 4. Radial profiles of current density during Experiments (a) 8, (b) 4, (c) 11, (d) 7, each 2 ms.

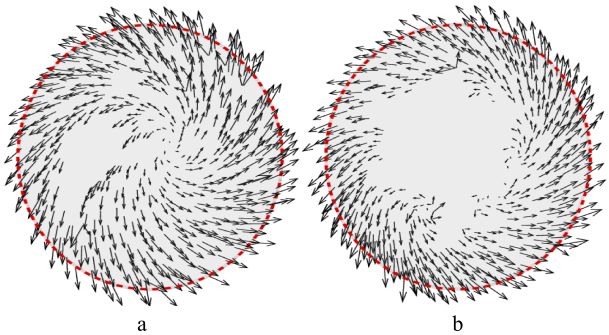

Figure 5. Calculated direction of retrograde motion with Robson drift of cathode spots during Experiments (a) 4 and (b) 11 at 4 ms.

1. At low current (Figure 4.a), the current density is approximately uniform up to 20 mm, and then decreases for higher radial positions. This decrease reflects that the circumference of the cathode is partly non occupied by the cathode spots. After the

current peak, the current density decreases approximately in uniform manner, confirming the previous comment made on Figure 3.

2. At higher currents (Figure 4.b-d), the radial profiles of the current density before the current peak are markedly different from that at low current. Due to the initial presence of spots over a large portion of the edge of the cathode, one observes a peak of current density at the cathode edge followed by a sharp fall towards the center of the cathode. As the current rises, the front of current density moves towards the center of the cathode. Nevertheless the current density does not exceed its maximal value reached at $t = 2\,\mathrm{ms}$. At the current peak, when the cathode is fully occupied, the current density is roughly uniform. After the current peak, the current density tends again to decrease uniformly over the surface.

4. Discussion

Figures 3.b-c suggest that the partial or total occupation of the cathode surface by CSs at moderate currents is related to the observed off-centered or centered position of the CS empty region, this characteristic being itself linked to the initial repartition of CSs along the cathode circumference. In Figure 5, based on the measured CS distribution, we have calculated the direction of motion of CSs, following a similar approach to that used in [10]. The plotted vectors represent the retrograde direction of motion associated to the self-generated azimuthal magnetic field, taking into consideration the Robson angular deflection of the motion caused by the AMF [11]. The deflection angle was defined as $\varphi_r = \eta \tan^{-1} \frac{B_{AMF}}{B_t}$ where $\eta \sim 0.8$ on CuCr30 cathode[10]. When the empty region is off-centered (Figure 5.a), the CS motion direction clearly contributes to the filling of the empty region. On the contrary, when the empty region is relatively centered (Figure 5.b), the CS motion direction points only little towards the empty region, which may explain the non-disappearance of this region.

5. Conclusion

The distributions of cathode spots and current density at the cathode in a long gap vacuum arc controlled with an external axial magnetic and ignited on the lateral surface of the cathode have been investigated.

- □ Various types of CS distribution were observed depending partly on the current. At low currents, CSs form a compact group which does not occupy completely the cathode surface, whereas at high currents the whole cathode surface is covered by CSs. At moderate currents, a CS empty region may subsist at the current peak, which may have its origin in the initial CS distribution along the circumference of the cathode following the arc ignition on the lateral surface of the cathode.
- □ The contact gap in the range considered in this paper seems to have no impact on the CS distribution.
- □ A value of the average current emitted by a cathode spot of $36.5 \pm 2.5\,\mathrm{A}$ has been determined.
- □ In regions occupied by CSs, the current density at the cathode seems roughly uniform.

Acknowledgements

This project was supported by the French Government in the framework of the "Investments for the Future" programme under the project reference (ANE-ITE-002-01).

References

[1] P. Picot. Vacuum switching. Technical Report 198, Schneider Electric, 2000.

[2] X. Song, Z. Shi, C. Liu, S. Jia, and L. Wang. Influence of AMF on the expansion speed of cathode spots in high-current triggered vacuum arc. *IEEE Trans. Plasma Sci.*, 41(8):2061–2067, 2013.

[3] L. Wang, S. Jia, Z. Shi, and M. Rong. Numerical simulation of vacuum arc under different axial magnetic fields. *J. Phys. D: Appl. Phys.*, 38(7):1034–1041, 2005.

[4] V.P. Afanas'ev, A.M. Chaly, A.A. Logatchev, S.M. Shkol'nik, and K.K. Zabello. Computer-aided reconstruction of the cathode images obtained by high speed in high photography of high current vacuum arcs. *IEEE Trans. Plasma Sci.*, 29(5):695–699, 2001.

[5] A.M. Chaly, A.A. Logatchev, K.K. Zabello, and S.M. Shkol'nik. High-current vacuum arc appearance in nonhomogeneous axial magnetic field. *IEEE Trans. Plasma Sci.*, 31(5):884–889, 2003.

[6] Z. Shi, S. Jia, X. Song, Z. Liu, H. Dong, and L. Wang. The influence of axial magnetic field distribution on high-current vacuum arc. *IEEE Trans. Plasma Sci.*, 37(8):1446–1451, 2009.

[7] A.M. Chaly, K.K. Logatchev, A.A. Zabello, and S.M. Shkol'nik. High-current vacuum arc in a strong axial magnetic field. *IEEE Trans. Plasma Sci.*, 35(4):939–945, 2007.

[8] B. Jüttner and I. Kleberg. The retrograde motion of arc cathode spot in vacuum. *J. Phys. D: Appl. Phys.*, 33(12):2025–2036, 2000.

[9] L. Yu, J. Wang, Y. Geng, G. Kong, and .Z Liu. High-current vacuum arc phenomena of nanocrystalline CuCr25 contact material. *IEEE Trans. Plasma Sci.*, 39(6):1418–1426, 2011.

[10] S. Jia, X. Song, Z. Shi, L. Wang, and X. Huo. Investigations on the motion of high-current vacuum-arc cathode spots under a magnetic field. *IEEE Trans. Plasma Sci.*, 39(6):1344–1348, 2011.

[11] A.E. Robson. The motion of low-pressure vacuum arc in strong magnetic field. *J. Phys. D: Appl. Phys.*, 11(13):1917–1923, 1978.